Honey bee associated viruses are unlikely to impact bumble bee colonies while habitat heterogeneity supports their resilience

Laura Bosco[1], Orlando Yañez[2], Alexandria Schauer[2], Corina Maurer[3], Samuel Cushman[4], Raphaël Arlettaz[3], Alain Jacot[5], Torsten Seuberlich[6], Peter Neumann[6], and Daniel Schläppi[2]

[1]Finnish Museum of Natural History
[2]University of Bern Institute of Bee Health
[3]University of Bern Faculty of Natural Sciences
[4]University of Oxford
[5]Swiss Ornithological Institute
[6]University of Bern

September 4, 2023

Abstract

Virus host shifts from managed honey bees, Apis mellifera, are thought to contribute to the decline of wild pollinators. However, data on the impact of such viruses on wild pollinators remain scarce, and how landscape structure may affect virus transmission is poorly understood. We experimentally deployed bumble bee colonies in an agricultural landscape to study changes in the bumble bee virome under varying habitat composition and configuration. The results show a decline in prevalence and viral loads of honey bee associated viruses, while viruses common in Bombus spp. increased during field exposure. Honey bee associated viruses had no effect on colony development, suggesting that immediate impacts are unlikely in the field. Notably, we further demonstrate that increased habitat diversity results in fewer viruses in Bombus colonies. To mitigate the decline of bumble bees and other wild pollinators, we suggest focusing conservation efforts on habitat diversification and restoration.

INTRODUCTION

Interspecies disease transmission can have profound impacts on human and animal health , as strikingly evidenced by the recent Covid-19 pandemic. Emerging infectious diseases have been linked with rapid declines of global entomofauna , where disease transmissions between domesticated animals and wildlife populations are of particular concern . Globally traded managed western honey bees (*Apis mellifera*) suffer from a range of emerging pathogens . Thereby, they may act as an important source of pathogens for wild arthropods with whom they share the environment . Overlapping ranges, niches and behaviors promote cross-species disease transmission . Thus, commercial pollinators have been mentioned as key drivers of disease emergence in other beneficial insects and pathogen spillover from honey bees is a possible cause for the decline of wild pollinators, including bumble bees (*Bombus*spp., .

RNA viruses have a high potential to cross species barriers due to their large population sizes and error prone replication that enable rapid adaptive change . Many (RNA) viruses that were first described in honey bees have been subsequently detected across the wider arthropod community . Based on the co-occurrence of viruses and shared viral strands within a site, frequent interspecific virus transmission is suspected, especially

between honey bees and bumble bees . In contrast to burgeoning evidence for the occurrence of honey bee associated viruses in other arthropods, knowledge on their impacts in alternative hosts is limited .

The few studies that investigated pathogenicity outside of honey bees report potential clinical symptoms in *Bombus* spp. (*Vespa crabro* , , ants (*Lasius niger* , , and spiders (*Agelena labyrinthica* , . However, except for wing deformities in field-observations – a clinical symptom associated with Deformed wing virus (DWV) – reports on pathogenicity are based on laboratory worst case scenarios with exposure (injection, feeding) to copious amounts of viral copies (e.g., . Thus, it remains unclear if pollinator populations in the field are affected by frequent exposure to viruses from managed honey bees, as claimed in the literature .

When investigating potential impacts of viruses on wild bee populations, it is important to consider additional stressors affecting their fitness and resilience. Among the most important drivers of current insect declines are habitat loss and fragmentation . Habitat loss and fragmentation often lead to homogenized landscapes poor in floral resources and, in consequence, lowered pollinator abundance and species diversity . Fragmented agroecological systems pose a particular challenge to biodiversity, not only in regards of their landscape composition and configuration, but also in terms of pollution through agrochemicals . Consequently, pollinators inhabiting such landscapes are inevitably faced with multiple intertwined stressors, which may reinforce each other's adverse effects . In fact, both nutritional stress and exposure to pesticides have been shown to impact honey bee immune pathways , potentially leading to synergistic stressor effects, as suppression of insect immune systems can increase pathogen susceptibility . Furthermore, habitat composition and configuration in fragmented landscapes influence transmission dynamics of infectious diseases via shared floral resources, which act as viral hotspots and are the most likely route for cross-species virus transmission among pollinators

The probability of susceptible hosts being exposed is likely increased in fragmented landscapes with limited and spatially clumped floral resources . Second, essential floral resources can increase the tolerance of the hosts to withstand pathogens , since the availability of high quality and diversity pollen and nectar resources positively influences bee health and reduces pathogen susceptibility . Hence, host responses to landscape structure or increased floral numbers, e.g., through altered foraging patterns or diet breadth (Gómez-Martínez et al. 2022), may shape pathogen prevalence and disease outbreaks in bee communities . While modelling suggests that benefits from floral resources, corridors and other connections may outweigh the possible risks of increased pathogen transmission , empirical studies linking landscape structure and disease transmission, and their impact on pollinator fitness, are lacking because controlled experimental manipulations of landscapes, target hosts and pathogens, are often infeasible .

Here, we take advantage of the intensive viticulture to study how landscape structure affects viral load dynamics in bumble bee field colonies, and how this is linked to colony development. More specifically, we asked i) how the composition of viruses in bumble bee colonies changes following exposure to the environment; ii) if and how the most dominant viruses are correlated with colony development; and iii) whether the landscape structure affects the viral load, richness, and turnover in bumble bee colonies.

MATERIAL AND METHODS

Study area and design

From May to June 2017, the study was conducted in Central Valais, Switzerland. The landscape is dominated by vineyards interspersed with small patches of dry oak stands, steppe and orchards in the plains. About 70-80% of the vineyards are intensively managed and support virtually no ground vegetation due to regular herbicide application, whereas the remaining 20-30% are cultivated by farmers who have adopted more environmentally friendly management practices, promoting ground vegetation . Forty *B. terrestris terrestris* colonies, purchased from Andermatt Biocontrol, were allocated to vineyard fields of varying ground-vegetation coverage, landscape composition and configuration in a semi-experimental factorial approach (Fig.

1; see Maurer et al. 2020).

Bumble bee colonies

Two-week-old colonies of *B. terrestris terrestris* were weighed as a proxy of initial colony size and then randomly allocated to experimental fields, where they remained from 08-May-2017 to 23-June-2017. Weight gain of colonies, number of workers, queens and total number of pupal cells (as a sum of healthy, dead and hatched pupal cells, pollen and nectar pots), as well as infections by parasitic moths, *Aphomia sociella* , were assessed. For details, please refer to Maurer et al. (2020). Workers (N = 5) were collected from 35 colonies at the start and at the end of the experiment, stored at -20°C until the transfer to the laboratory and then stored at -80°C until further processing.

Environmental predictors

To assess the role of the composition and configuration of major land-use types around the experimental fields, we used the Swiss landcover data SwissTLM3D (copyright@swisstopo 2020, resolution 1-3m). As not all municipalities were covered by this data, we additionally used the CORINE landcover data from 2018 to fill the gaps (© European Union, Copernicus Land Monitoring Service 2020, European Environment Agency EEA). We then aggregated the landcover classes (Fig. 1, see SI section 1.1 for details on class aggregation) and calculated the relative area covered by farmland, forests, residential areas, and vineyards within 9 buffer zones ranging from 100 m up to 1'500 m radii in 100 m increments (100–500m) and 250 m increments (500–1'500m), respectively (see SI Fig. S1). To do so we used the metric percentage of landscape (PLAND, in the R package landscapemetrics (Hesselbarth et al. 2019). We also calculated the mean distance between patches of the same landcover class as a measure of configuration (mean of Euclidean nearest-neighbor distance ENN_MN). Lastly, we obtained an estimate of landscape heterogeneity for the same 9 spatial scales by calculating a Shannon diversity index based on all eight reclassified land-cover classes, taking both the number of land-cover classes and the abundance of each class into account (metric Shannon diversity SHD). We additionally calculated habitat area (PLAND) and fragmentation (patch density, PD) of vegetated vineyard fields specifically within the same 9 spatial scales as it has been shown to be an important landscape feature for arthropods, including bumble bees .

To investigate field-scale effects of vineyard management on virus susceptibility of bumble bees, the ground vegetation density and flower resources were measured during the period of experimentation in a random subset of 6 vegetated vineyard fields surrounding the experimental field within a buffer zone of 250 m radius (see . Additionally, we included the field size of the experimental field as an explanatory variable (Table 1).

To address the influence of honey bee hives in relation to virus transmissions in the surroundings of the bumble bee colonies, we included the nearest-neighbor distance to the next honey bee hive and the number of honey bee hives within the 9 spatial scales. All these metrics were calculated in R

Virus analyses

RNA extraction – For the virus identification RNA was extracted from bumble bees (N = 5 per colony) collected at the beginning (day 0) and at the end of the experiment (day 45) using a NucleoSpin® RNA II kit (Macherey-Nagel, Oensingen, Switzerland) following the manufacturer's recommendations. Individual bees were crushed in PBS Buffer (0.5 mg tissue/µL) with a 5-mm metal bead in 2-mL Eppendorf® (Basel, Switzerland) tubes using a Retsch® (Haan, Germany) MM 300 mixer mill for 1 min at 25 Hz . Fifty µL of the homogenate was used for the extraction and RNA got stored in 60 µL elution buffer .

Next generation sequencing – RNA from every colony was used for the identification of bee viruses present in the bumble bee colonies. Briefly, after QC evaluation, RNA from each individual was pooled according to the two sampling sessions (day 0 and day 45). Libraries comprising each sampling session were prepared

using the Corall total RNA-Seq Library kit (Lexogen, Vienna, Austria). NGS were performed using an Illumina SP flow cell (100 Mio reads/pool, 300 cycles) in paired-end mode (2 × 150 bp).

Bioinformatics analysis – Reads were quality-trimmed with fastp Version 0.12.5) and mapped to the Bombus terrestris host genome (iyBomTerr1.2, ncbi bioproject PRJEB45694) using STAR Version 2.7.3a). Quality-trimmed and unmapped reads were assembled via SPAdes Version 3.14.0). Resulting scaffolds were then aligned to virus nucleotide and protein and sequence databases (Genbank and RefSeq viral nucleotide sequences downloaded on 21-01-2021, UniProt viral amino acid sequences downloaded on 21-01-2021) using BLASTn , Version 2.0.0+, default settings) and DIAMOND , Version 0.9.18, default settings). To exclude false positives, the scaffolds with a virus hit were aligned to an in-house non-viral database consisting of archaeal, bacterial, fungal, mammal, and protozoal sequences. Scaffolds were considered false positive if they had a longer hit on a sequence of the in-house database compared to the virus databases or if they had a nucleotide hit of more than 10% of their own length to any sequence of the non-viral database.

Reverse transcription and quantitative PCR (RT-qPCR) – cDNA synthesis was performed for each sample (pooled RNA from 5 individuals from each colony) using a M-MLV RT Kit (Promega, Dubendorf, Switzerland). In brief, a thermocycler (Biometra, Analytik Jena, Jena, Germany) was used to incubate 0.75 µL of a random hexamer oligonucleotide (100 µM) and H2O for 5 Minutes at 70 °C with 0.5 µg of template RNA. Then, 5 µL of 5x buffer, 1.125 µL dNTPs (10 mM) and 1 µL reverse transcriptase (M-MLV) were added followed by incubation at 37 °C for 60 min. For the virus quantification, the group of bee viruses with the highest number of reads from the above-described libraries were selected (SI Table S1). qPCR reactions were prepared using 6 µL of 2X reaction buffer (SensiFAST SYBR® No-ROX Kit, Meridian Bioscience, London, UK), 0.24 µL forward and reverse primer (SI Table S2), 2.52 µL water and 3 µL of ten-fold diluted cDNA. The qPCR reactions were performed in a CFX96TM Real-Time PCR Detection Systems (BioRad, CA, USA) with the following conditions: 3 min for 95°C, 40 cycles of 3 sec at 95°C and 30 sec at 57°C. The amplification was followed by a melting curve analysis of the strand dissociation to verify product specificity. The analysis was performed by reading the fluorescence at 0.5 °C increments from 55 to 95 °C. Each sample was run in duplicate for each of the targeted virus and the Rps5 reference gene. Furthermore, each plate was run with a ten-fold serial dilution of purified PCR products that served as standard curves and two no-template negatives .

Statistical Analyses

We used the viral load of the nine screened viruses to calculate total viral load (number of virus genome copies). Viral loads were first log transformed and then summed up per colony and sampling session (day 0 and day 45) to calculate the total viral load. To answer the first research question regarding how the viral load, richness and viral loads of the viruses changed from before to after the field exposure, we ran linear models with total viral load, virus richness, and viral loads of the six most abundant viruses (Deformed wing virus-B DWV-B, Black queen cell virus BCQV, Castleton burn virus CBV, Mayfield virus-1 MV 1, Duke bunyavirus DBV, Bombus cryptarum densovirus BcDV) as response variables against the session (i.e. day 0 versus day 45).

To test the effects of initial viral loads on colony development parameters (research question ii) we used initial viral load (day 0), and viral loads of the same six most abundant viruses in single-predictor linear models. The following eight colony development parameters were used: number of workers, number of queens, number of total cells, number of hatched pupal cells, weight gain, moth infestation index, and number of parasitic larvae or pupae.

Next, the influence of landscape structure on the virome change was assessed (research question iii). For this purpose, change in virus loads was calculated as$(\log(\,viral\ load)_{day\ 45} - \log(viral\ load)_{day\ 0})$for total virus load or for each of the six most abundant viruses separately. Similarly, for the change in virus richness, we calculated the number of viruses present at day 45 – the number of viruses present at day 0. For the turnover and appearance of viruses during the field exposure we used the function 'turnover' (package codyn, .

For each of those response variables, we first ran single-predictor models for each explanatory variable separately (see Table 1), using simple linear models given the normal distribution of residuals. For all explanatory variables, those with p<0.1 were combined in a full model. For predictors that were measured at multiple spatial scales, one model per scale was run. If (near-)significant effects (p<0.1) were found, the best scale based on lowest AIC was selected for the full model. Thus, variables could enter the full model at different scales – following a multi-scale analytical framework . Before running the full model, collinearity among predictors was checked with a threshold of Pearson<0.6. For collinear variables, the one with higher AIC in the single-predictor model was dropped from the full model. For the full models, we did a stepwise backwards selection until only (near-)significant variables were left in the model. Among those candidate models, the best one was selected based on best model performance, which was checked using 'compare_performance' (package 'performance' . Additionally, we correlated colony development parameters with the field and landscape variables (see detailed methods and results in SI section 3). Model assumptions such as normality of residuals, homoscedasticity, and outliers were checked (package 'performance'). Spatial autocorrelation of model residuals was tested for each model using the function 'testSpatialAutocorrelation' (package DHARMa, All data and code are available from zenodo online repository (Bosco et al. 2023).

RESULTS

Change in virus composition before and after exposure to the environment

Overall, the most prevalent viruses in the bumble bee colonies were DWV-A, DWV-B, BQCV, LSV, ARV-1, which are all honey bee associated viruses . In addition, several bumble bee associated viruses were abundant: BcDV, CBV and MV 1 . Total viral load across all viruses (log scale) increased on average by 1.34±2.21 (mean±SD) from the beginning to the end of the field exposure (day 0 = 3.67±1.47; day 45 = 5.00±1.61; lm: estimate±SE = 1.335±0.368, p<0.001), while total virus richness on average increased by a factor of 1.46±1.75 from day 0 to day 45 (day 0 = 3.14±1.03; day 45 = 4.60±1.31; lm: 1.457±0.282, p<0.001). Among the 9 screened viruses, only 1 to 5 were present at day 0, whereas at day 45 between 2 and 7 viruses were present among the colonies (Fig. 2).

The generally large increase in viral richness from day 0 to day 45 was driven by the appearance of new and mostly bumble bee specific viruses, such as CBV (lm: 2.852±0.467, p<0.001) or the MV 1 (lm: 2.291±0.404, p<0.001) as well as the DBV (lm: 3.006±0.309, p<0.001). At day 0 colonies had either viral loads dominated by the BcDV (significant increase; lm: 0.804±0.376, p = 0.036) or a combination of two honey bee viruses: DWV-B (significant decrease; lm: -0.990±0.363, p = 0.008) and BQCV (significant increase; lm: 0.639±0.198, p = 0.002; Fig. 2, SI Fig. S2).

Influences of initial colony viral loads on colony development

Among all measured colony development parameters, only the moth infestation index was related to the initial viral loads of viruses, with increasing loads of DWV-B colonies were related to higher moth infestation rates at the end of the field exposure (estimate±SE=0.210±0.081, p=0.012), while increasing BcDV loads led to fewer moth infestations (-0.218±0.079, p=0.008; SI Table S3).

Change in viral patterns in relation to landscape structure

Total Viral Load Change – The mean distance among forest patches (1250 m radius) had a marginally significant and positive relationship with the total viral load change in bumble bee colonies, while mean distance among agricultural patches showed a large positive and significant relationship (Table 2A, Fig. 3a), meaning that bumble bee colonies located in more isolated (or less connected) agricultural patches had a higher increase in viral loads during the field exposure (SI Fig. S3a).

Virus Richness Change – Habitat diversity (300 m), a measure of landscape heterogeneity, was significantly negatively related to virus richness change, showing that bumble bee colonies placed in areas with fewer different habitat types (lower heterogeneity) were infected with a higher number of different viruses after field exposure (Table 2B, Fig. 3b). On the other hand, forest area (100 m) was significantly positively related to virus richness change; with increasing forest cover within the close surroundings of a colony, the number of viruses infecting the colony increased (Table 2B; SI Fig. S3b, c).

Virus Turnover – The area covered by forests (100 m) had the strongest effect on viral turnover. Colonies in areas with more forest showed a higher change in their virus composition (Table 2C). However, with increasing distances (decreasing connectivity) among forest patches (400 m), virus turnover also increased significantly. Also, fragmentation of vegetated vineyards (400 m) significantly influenced the turnover, such that the viral composition changed less for colonies in areas with higher fragmentation (Table 2C; SI Fig. S4a-c).

Virus Appearance – Habitat diversity and forest area both were significantly related to virus appearance, with habitat diversity (300 m) again showing a negative effect, such that colonies in areas with a lower number of different habitat types were more frequently infected with viruses that were not yet present at the beginning of the field exposure. Increasing forest area within the wider surrounding of a colony (500 m) led to the appearance of new virus infections (Table 2D; SI Fig. S4d, e).

Overall, among the different spatial scales tested (ranging from 100 m to 1500 m), the predictors included in the final models had their strongest influence on the different response variables within smaller scales (100 m to maximum 500 m), indicating that the pattern of viral infections in bumble bee colonies influenced by the landscape is influenced by local rather than meso- or landscape scale heterogeneity.

Regarding the responses of colony development parameters to the landscape and field structure, we found very similar responses as for the viral patterns with generally positive relationships with agricultural or residential areas and habitat diversity but negative links to forest cover and connectivity. For detailed results see SI section 3.

DISCUSSION

In this study we investigated changes in the bumble bee virome under field conditions in relation to habitat composition and configuration. Our results show that viral loads and viral richness increased after field exposure and shifted from an initial dominance of honey bee associated viruses to a higher virus richness in the colonies at the end of the experiment, including several different bumble bee viruses. The spatial structure of the surrounding landscape was related to the changes in viral patterns at fine spatial scales, with habitat Shannon diversity being positively linked to lower virus richness and appearance of new viruses, while well-connected agricultural patches decreased the viral load. Colony development parameters were not directly negatively affected by viruses but were influenced by the same landscape parameters that drove virus prevalence. Our results emphasize the importance of landscape heterogeneity and connectivity for wild pollinator health .

Change in virus composition before and after field exposure

We show that the bumble bee colonies were initially mainly infected with either honey bee viruses (DWV-B and BQCV) or the bumble bee virus BcDV, while after field exposure bumble bee viruses (CBV and MV 1) joined the group of the most prevalent viruses in the new virome composition. DWV-B, initially highly prevalent in the colonies, could not be detected in the study colonies after field exposure. This result was unexpected as DWV is regarded as an emerging infectious disease commonly responsible for the elevated viral loads found in honey bees (the reservoir host, Tehel et al. 2020) and it is assumed the spill-over of this virus may negatively impact wild bee species . However, the lower prevalence detected after field exposure could be related to bumble bees being inefficient hosts for DWV. Tehel et al. 2020 showed, under laboratory

conditions, that the inoculation of DWV by injection produces lower viral replication in *B. terrestris* than in honey bees, even though bumble bees are bigger in body size. Moreover, *B. terrestris* showed considerable resistance to DWV infection when fed orally (Gusachenko et al. 2020). Since the oral-fecal route is the main virus transmission route between bees , limited oral transmission would contribute against the quick distribution of this virus among the colonies and may help to explain the low DWV prevalence in our experimental colonies. However, corresponding to the seasonal peak of Varroa destructor mites in honey bee colonies, the spill-over of DWV from managed honey bees can be expected to peak in late summer (, which is after the bumble bee colonies were exposed to the field.

In contrast, viruses related to bumble bees (BcDV, CBV and MV 1) were largely prevalent after field exposure. Those viruses have been reported in several bumble bee species such as *Bombus cryptarum* , *B. terrestris* , *B. pratorum* , and *B. pascuorum* suggesting their close association with the taxon. Within a host, viruses are in competition with each other. Better adapted viruses should outcompete their counterparts and establish themselves , which could explain the observed shift towards bumblebee associated viruses. This indicates that these viruses might be well adapted to bumble bee hosts rendering them transmission advantages. However, more studies are necessary to determine the true host range of those viruses. In general, the decreasing trends in prevalence and viral loads of honey bee associated viruses suggests that, in contrast to previous claims, virus host shifts from managed honey bees to bumble bee colonies may often have limited impact on the latter under field conditions. However, the current study was not designed to address carry over-effects. The production of new queens and drones, as well as hibernation and colony initiation success of gyns, were not assessed and thus long-term impacts on populations cannot be excluded.

Notably, the virus infections were mostly inconsequential to the performance or health of the colonies. The number of workers, queens, brood cells and hatched pupal cells, as well as weight gain, important colony development parameters that serve as proxies for fitness, remained unaffected. Interestingly, elevated initial DWV-B loads were associated with heightened rates of moth parasitism, whereas higher initial BcDV loads coincided with decreased moth infection rates. Hence, our results remain inconclusive regarding whether virus infections modulate susceptibility for other parasites in bumble bees. As a result of parasite-induced immunosuppression reducing the immune capacity of a host organism, co-infections may be beneficial to one or multiple parasites, facilitating subsequent infections . Conversely, interactions may be antagonistic to at least one of the parasites due to resource competition or cross-effective immune responses . These findings highlight the challenges of comprehending multi-species interactions and underscore the possibility of incorrect risk assessment when investigating parasite impacts in isolation, rather than considering the broader context of pathogen communities .

Landscape structure influences viral infection patterns

Our data show that colonies located in habitats with more floral resources, (e.g., agricultural or residential areas), generally have lower viral load and richness. This aligns with previous research that has demonstrated a connection between higher amounts of floral resources and reduced pathogen loads in pollinators . Moreover, colonies in areas with low isolation of agricultural patches had lower total viral load and colonies in more heterogeneous (i.e., diverse) areas had a lower number of different viruses as well as a lower probability to be infected with new viruses. Agricultural patches, mainly consisting of vegetated vineyards, orchards and grasslands, along with their field edges, provide suitable floral resources . This suggests that high habitat diversity might result in a higher chance of finding suitable and diverse floral resources, providing resource complementation .

Consequently, habitat heterogeneity might reduce virus transmission via three non-mutually exclusive mechanisms shaping fitness and foraging patterns of bees: (i) High floral resource availability and resource complementarity due to landscape heterogeneity increase general colony performance and health and thereby decrease their susceptibility to pathogens (Roger et al. 2017), (ii) high floral abundance within a landscape may decrease the contact between pollinators simply because pollinators are not concentrated on the few available flower patches (dilution/amplification effect) and (iii) high habitat/floral diversity can modify a species diet breath with consequences on virus transmission .

We further show that colonies located in areas with a higher cover of forests were infected with more viruses (higher virus richness) and showed increased virus turnover and appearance of new viruses. *B. terrestris* generally prefer open habitats. Consequently, forests do not provide suitable foraging grounds and may even constitute landscape barriers to foraging bumble bees . Thus, a higher forest proportion in the landscape may reduce foraging resources and lead to lower colony fitness through poorer nutrition and/or higher viral spillover rates as foraging bees are concentrated in the remaining suitable patches .

Overall, the landscape structure effects operated at rather fine scales, ranging from 100 up to a 400 meter radius around the bumble bee colonies, indicating that the habitat structure of the immediate surroundings is more important than meso- or large-scale conditions . Even though B. terrestris have been shown to forage over long distances their main foraging activity occurs within 70-600 m around the colonies supporting the findings in this study.

CONCLUSIONS

This study highlights that even though commercially raised bumble bees typically carry several honey bee viruses, the viral composition generally changes towards bumble bee viruses after field exposure, with no or little impact on colony development. Hence, the widely studied and discussed negative impacts of honey bee virus transmissions to wild pollinators might often be negligible for *B. terrestris* since neither a coherent establishment of such viruses in the colonies during field exposure nor clear consequences on colony development were found. Additionally, our results highlight the importance of landscape structure in shaping viral patterns during field exposure. Notably, habitat heterogeneity and well-connected agricultural patches in areas with little forest cover led to lower viral loads, fewer viruses, and lower appearance of new viruses in bumble bee colonies. We thus highlight the importance of habitat diversity and heterogeneity in agricultural landscapes, as evidenced numerous times before underline the importance of maintaining existing heterogeneous agricultural landscapes and restoring where necessary.

Acknowledgements:

We thank all farmers and the VITIVAL (Valais association for viticulture) groups for their collaboration and allowing us to do this study on their vineyards. We are grateful to Elisabeth Klaus, Beatrice Schranz and Franziska Arnold for field and lab assistance. To Michael Koch for the bioinformatic support. Financial support was granted by the Swiss National Science Foundation to Alain Jacot (31003A_149780) and to D.S. (P500PB_206883) and to P.N. by the Béatrice Ederer-Weber Foundation and the Vinetum Foundation.

REFERENCES

TABLES

Table 1. All initial covariates, their description, data types, scales, and mean ± standard deviation SD. For variables measured at the nine spatial scales (mean ± SD) are given for the intermediate 750-meter radius scale. PLAND = percentage of landscape; PD = patch density; NND=Nearest-Neighbor-Distance; BB = Bumble bee colonies; HB = Honey bee colonies; MS = Multiscale.

Covariate	Description	Data type/source
Vineyard field		
Vegetation	Ground vegetation density (%)	Field estimate*
Flower species richness	Mean number of flowering plant species	Field estimate*
Nr flowers	Mean density of flowering plants	Field estimate*
Field size	Area of vineyard field (m^2)	QGIS

Covariate	Description	Data type/source
Landscape composition/ configuration	*Landscape composition/ configuration*	*Landscape compositio*
Vegetated vineyard area	PLAND of vegetated vineyards (%)	FRAGSTATS
Vegetated vineyard fragmentation	PD of vegetated vineyards	FRAGSTATS
Vineyard area	PLAND of vineyards (%)	FRAGSTATS
Residential area	PLAND of residential areas (%)	FRAGSTATS
Mean distance residential	NND between residential areas (m)	FRAGSTATS
Forest area	PLAND of forests and groves (%)	FRAGSTATS
Mean distance forests	NND between forests and groves (m)	FRAGSTATS
Farmland area	PLAND of farmland (%)	FRAGSTATS
Mean distance farmland	NND between farmland patches (m)	FRAGSTATS
Habitat diversity	Shannon diversity of habitat types within the landscape	FRAGSTATS
Bumble bee colonies	*Bumble bee colonies*	*Bumble bee colonies*
Nr workers	Number of workers per colony	Lab dissection*
Nr queens	Number of queens per colony	Lab dissection*
Nr cells	Number of total cells per colony	Lab dissection*
Nr pupal cells	Number of hatched pupal cells per colony	Lab dissection*
Colony weight change	Weight gain of colonies (mg)	Lab dissection*
Moth infestation rate	Severity of moth infestation in the colony	Lab dissection*
Nr parasitic larvae or pupae	Number of parasitic larvae or pupae per colony	Lab dissection*
Honey bee colonies	*Honey bee colonies*	
Distance to HB	Nearest-neighbor distance to honey bee hives (m)	QGIS
Nr HB colonies	Number of honey bee hives around the bumble bee colonies	QGIS

** from Maurer et al. 2020*

Table 2. Model outputs of best models for A) change in total viral load, B) change in virus richness (number of viruses present), C) turnover of viruses from start to end of the experiment, D) appearance of new viruses from start to the end of the experiment. Estimates, standard errors (SE), p-values, and confidence intervals (CI) from linear models (lm) are given. N = 35 observations (1 observation per bumble bee colony) for all models. NND = nearest-neighbor distance (mean distance between patches of same landcover type); PLAND = percentage of landscape (relative area covered by landcover type); PD = patch density (number of separate patches per 100 ha of same landcover type).

Variable	Estimate	SE
Change of total viral load (log), R^2 = 0.298	*Change of total viral load (log), R^2 = 0.298*	*Change of total viral load (log)*
Intercept	**1.335**	**0.312**
NND forests 1250 m	0.591	0.320
NND agricultural 400 m	**1.059**	**0.320**
Change in virus richness, R^2 = 0.280	*Change in virus richness, R^2 = 0.280*	*Change in virus richness, R^2 =*
Intercept	**1.457**	**0.252**
Habitat diversity 300 m	**-0.721**	**0.285**
PLAND residential 100 m	-0.318	0.279
PLAND forest 100 m	**0.667**	**0.262**
Turnover of viruses, R^2 = 0.479	*Turnover of viruses, R^2 = 0.479*	*Turnover of viruses, R^2 = 0.4*
Intercept	**0.702**	**0.017**
PD vegetated vineyards 400 m	**-0.057**	**0.017**
PLAND forests 100 m	**0.071**	**0.017**
NND forests 400 m	**0.058**	**0.018**
Appearance of viruses, R^2 = 0.461	*Appearance of viruses, R^2 = 0.461*	*Appearance of viruses, R^2 = 0*

Variable	Estimate	SE
Intercept	**0.467**	**0.021**
Habitat diversity 300 m	**-0.074**	**0.024**
PLAND residential 100 m	-0.043	0.023
PLAND forests 100 m	**0.088**	**0.023**
NND forests 500 m	0.034	0.022

FIGURES

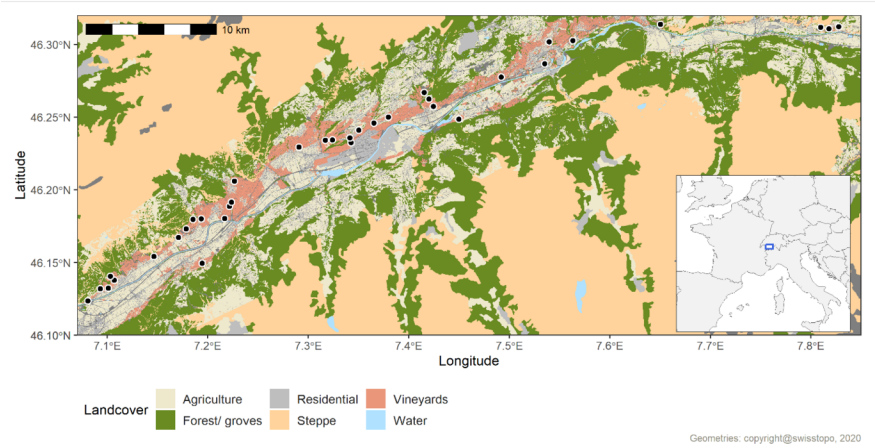

Fig. 1. Study area in Switzerland with 35 bumble bee colony locations (black dots) placed in the mosaic landscape of vineyards, other agriculture, residential areas, forests, and steppe.

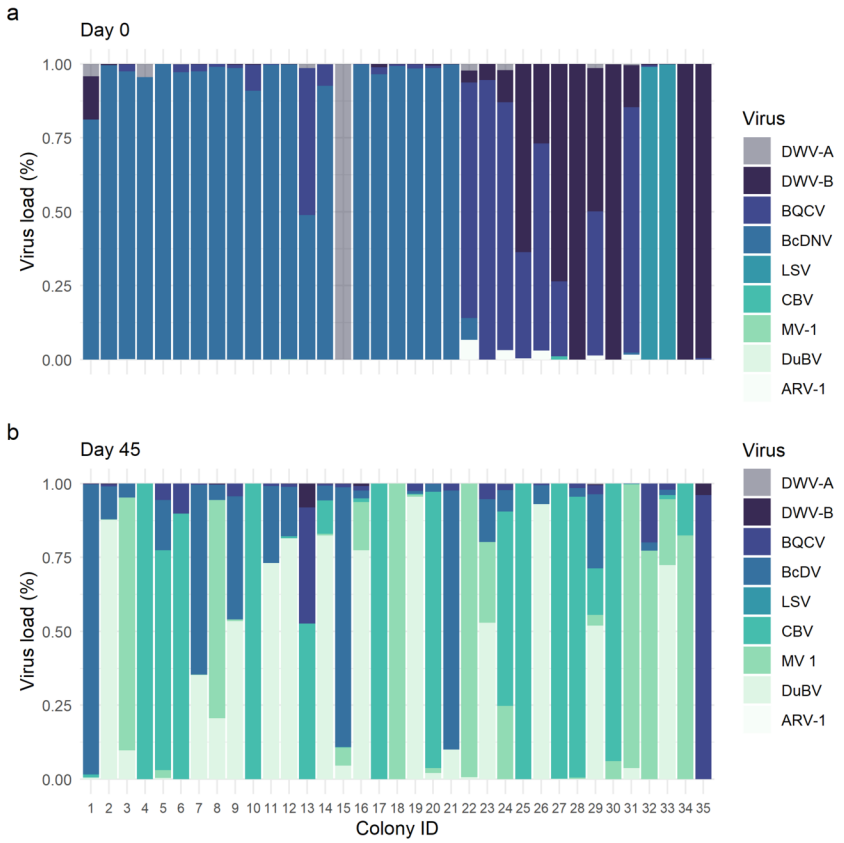

Fig. 2. Relative viral loads per bumble bee colony (x-axes) for the most prevalent viruses present at a) the beginning of the experiment, and b) the end of the experiment. DWV-A: Deformed wing virus A, DWV-B: Deformed wing virus B, BQCV: Black queen cell virus, LSV: Lake Sinai virus, ARV-1: Apis Rhabdovirus-1, BcDV: Bombus Cryptarum densovirus, CBV: Castleton Burn virus, MV 1: Mayfield virus 1, DuBV: Duke bunyavirus.

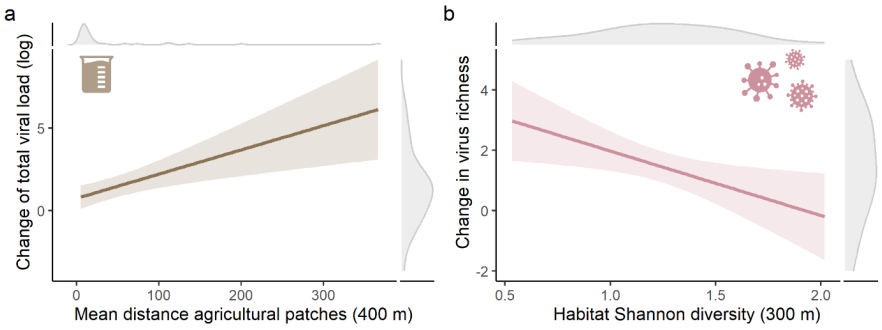

Fig. 3. Linear relationship between a) the change of total viral load (on the log scale) and the mean nearest-neighbor distance among agricultural patches within 400 m radius, and b) the change in virus richness and habitat Shannon diversity within 300 m radius around the bumble bee colonies. Estimates are derived from the respective best model per response variable where other terms present in the model were set at their mean. Solid line depicts the estimated mean, shaded area the confidence interval and the density

distributions at the right and top of the plot show the distribution of the raw data.

Hosted file

`Appendix S1.docx` available at https://authorea.com/users/520419/articles/663339-honey-bee-associated-viruses-are-unlikely-to-impact-bumble-bee-colonies-while-habitat-heterogeneity-supports-their-resilience